Supplementary Material

Supplementary Figure Legends

Supplementary Figure 1:

Representative RNA gel shows the quality of RNA samples labelled as "nd/ok" samples in Supplementary Table 1.

Supplementary Figure 2:

(A-B) Overall number and percentage of proliferating α-amylase-positive cells in the different phases of inflammation in WT and *Kras*^{G12D} pancreata; (B-C) Percentages of proliferating Sox-9-positive and Pdx1-positive cells in the different phases of inflammation in WT and *Kras*^{G12D} pancreata; *: $p<0.05$.

Supplementary Figure 3

(A-B) Number and percentage of proliferating Pdx1-positive cells in WT and *Kras*^{G12D} pancreata; (C) Representative IF of proliferating Pdx1-positive cells in WT (upper panel) and *Kras*^{G12D} (lower panel) pancreata in different phases of inflammation; scale bars: 50 µm.

Supplementary Figure 4

Percentages of proliferating αSMA-positive cells in different phases of inflammation in WT and *Kras*^{G12D} pancreata; *: $p<0.05$.

Supplementary Figure 5:

(A) Heatmap of the representative genes selected for the QRT-PCR verification in WT and *Kras*^{G12D} pancreata; (B) QRT-PCR data shows the expression of exocrine genes including Amy1, Try4, Pnlip and Krt19 in WT and *Kras*^{G12D} pancreata; (C) QRT-PCR data shows the expression of exocrine differentiation-related transcription factors including Bhlha15, Rbpjl, and Rbpj in WT and *Kras*^{G12D} pancreata; (D) QRT-PCR data shows the expression of mesenchymal genes including Tnc, Timp1, and Tnfrsf12a in WT and *Kras*^{G12D} pancreata; (E) QRT-PCR data shows the expression of inflammatory cytokines including IL6 and TNFα in WT and *Kras*^{G12D} pancreata; (F) QRT-PCR data shows the

expression of metabolism-related genes including Gpx2 and Tdh; relative expression obtained from at least three independent samples per group; *: $p<0.05$; (G-H) Representative IHC pictures show Tnc-positive and Gpx2-positive cells in the inflammation phase of WT, as well as in the lesions of early carcinogenesis (scale bars: 20 µm).

Supplementary Figure 6:

(A) Clustered heatmap of the inflammation phase gene signature allows differentiation of early carcinogenesis from control samples; (B) Heatmap of the inflammatory signature in normal pancreas, PanIN lesions, and advanced murine PDACs.

Supplementary Figure 7:

(A-C) Serum measurements show the time-dependent changes in the level of serum lipase, SAA, and CRP in the different phases in WT and $Kras^{G12D}$ pancreata.

Supplementary Figure 8:

(A-D) Flowchart of bioinformatic analysis techniques.

Supplementary Figure 9:

(A) Heatmap of 8 genes linked to activation of pancreatic fibroblasts in vivo; voxel colour: transcriptional up-regulation (red) and down-regulation (blue) as compared to the mean; each voxel indicates gene activity in one mouse sample arranged in chronological order; coloured bar: different phases in WT and $Kras^{G12D}$ samples, respectively; (B-C) Representative IHC pictures show Gli1-positive and Postn-positive cells in the mesenchymal compartment of early carcinogenesis (scale bars: 20 µm).

Supplementary Figure 10:

(A) Representative IHC pictures show Fgfr1-positive acinar cells in the acute phase of WT pancreata (scale bars: 20 µm); (B) QRT-PCR data show the expression of Amy2a3, Bhlha15 and Rbpjl in AR42J

cells after treatment with an Fgfr inhibitor (FIIN 1 hydrochloride (10 μM)) or dexamethasone (DEXA, 5 nM) for 72 hours; DEXA was used as the positive control; relative expression obtained from at least three independent experiments *: $p<0.05$; (D) QRT-PCR data shows the expression of Amy2a3, Bhlha15 and Rbpjl in AR42J cells after treatment with Fgf2 (50 ng/ml) for 72 hours (upper panel); relative expression obtained from at least three independent experiments *: $p<0.05$;

Supplementary Figure 11:

(A) Schematic illustration shows G0, G1, G2-X and G2-Z events in MADM lines; (B) Representative double-IF pictures show double positivity of GFP and Myc (scale bars: 200 μm); (C) Representative p-Erk, α-SMA and BrdU stained sections show expression of p-Erk, α-SMA and BrdU in PanIN lesions of inflammation-MEKP mice, scale bars: 20 μm.

Supplementary Methods

Mouse breeding

Mouse breeding was performed and husbandry was maintained at the specific pathogen-free mouse facility at the Technical University of Munich. The compound transgenic mice were maintained on a mixed background. All mouse experiments and procedures were approved by the Institutional Animal Care and Use Committees of the Technical University of Munich. All procedures were in accordance with the Office of Laboratory Animal Welfare and the German Federal Animal Protection Laws.

Primer sequences

Sequences of primers used for QRT or RT-PCR analysis of mouse genes:

Gene Name	Sense (5'→3')	Antisense (5'→3')
Amy1-m	CGAGAACTACCAAGATGCTGCT	TCCATCCCACTTGCGCATAA
Try4-m	AAGTCCCGCATCCAAGTGAG	CAAAGCTCAAGGTGTTGCCC
Pnlip-m	GACGGGATCTGGGAAGGAAC	CAAAGCCAGTTGGGTTGACG
Krt19-m	CCCAGGTCGCCGTCCACTCTGAGC	GCGTGCCTTCCAGGGCAGCTTTCATG

	A	C
Bhlha15-m	TCCCCAGTTGGAAGGGCCTCA	TCCTGCATGGGTGTTCGGCG
Rbpjl-m	GTATCGAAGTCAGTGGCGGT	GCAGGCTCAGGTGAGTCAAA
Rbpj-m	ACTGTAAGTGCCACTGCGAA	ACAACGGAACTGCAAACTGC
Tnc-m	TCGCAACTGGAAGGCCTATG	CCCTTGGGCTGTGATTTTGC
Timp1-m	CTTCTTGGTTCCCTGGCGTA	AGGACCTGATCCGTCCACAA
Tnfrsf12a-m	AGTCTGGTCCTGGTTTTGGC	TCACTGGATCAGTGCCACAC
Il6-m	GTGGCTAAGGACCAAGACCA	TAACGCACTAGGTTTGCCGA
Tnfα-m	ACCGTCAGCCGATTTGCTAT	CTCCAAAGTAGACCTGCCCG
Gpx2-m	CAGGGCTGTGCTGATTGAGA	GGGTAGGGCAGCTTGTCTTT
Tdh-m	TAGATTTTCGGTGCCTGCGT	TGGCGCTGATGTTGTAGGTT
Ptf1α-m	CTTGCAGGGCACTCTCTTTC	CGATGTGAGCTGTCTCAGGA
Nkx6-1-m	TTGCAAACTCTCTGGGTCGG	TGCGCAGCAAAAATGTCCAA
Rpl5-m	GGAAGCACATCATGGGTCAGA	TACGCATCTTCATCTTCCTCCATT
Rps29-m	TCTACTGGAGTCACCCACGGAA	GGAAGCACTGGCGGCACA

Sequences of primers used for QRT-PCR analysis of the rat genes:

Gene Name	Sense (5'→3')	Antisense (5'→3')
Amy2a3-R	ACTTGGCACAGTTATTCGCA	TGTCCACAAACACAAGGGCT
Bhlha15-R	GATGCCGACTTGGACATTGC	CACACTCCAGTTTGGCTCCT
Rbpjl-R	GGCCTCTTCAGACCATGTCC	CAGAGCCTGGCATCCGTTAT
Rbpj-R	AGACCCACGGTGTATTTCAGC	CAGTGTTCCGCTCTGCAACT
Ptf1α-R	CTACGAAAAGCGCCTCTCCA	GCCTCGATGGCAGATGATGA
Gapdh-R	GTTACCAGGGCTGCCTTCTC	GATGGTGATGGGTTTCCCGT

List of antibodies

Primary antibodies

Antibody name	Catalog number	Application* (Reactivity**)	Producer
Mouse Anti-BrdU Ab#	5292	IF (M)	Cell Signaling Technology
Rabbit Anti-FGF Receptor 1 mAb#	9740	IHC (M)	Cell Signaling Technology
Mouse Anti-Amylase Ab#	sc-46657	IF (M)	Santa Cruz Biotechnology (Heidelberg, Germany)
Rat Anti-BrdU Ab#	sc-56258	IF (M)	Santa Cruz Biotechnology
Rabbit Anti-Pdx1 pAb#	ab47267	IF (M)	Abcam (Cambridge, UK)
Mouse Anti-Sma-alpha Ab#	M0851	IF (M)	Dako Deutschland GmbH (Hamburg, Germany)
Rabbit Anti-Sox9 pAb#	AB5535	IF (M)	Merck Millipore (Billerica, MA, USA)
Mouse Anti-Tnc Ab#	NB110-68136	IHC (M)	Novus Biologicals (Cambridge, UK)
Rabbit Anti-Gpx2 pAb#	NBP1-32002	IHC (M)	Novus Biologicals
Rabbit Anti-Gli pAb#	NB600-600	IHC (M)	Novus Biologicals
Rat Anti-CD45 Ab#	550539	IHC (M)	BD Bioscience, Heidelberg, Germany
Rabbit Anti-Periostin pAb#	AP08724AF-N	IHC (M)	Acris Antibodies (Herford, Germany)

Secondary antibodies

Antibody name	Catalog number	Application*	Producer
Rabbit HRP (horseradish peroxidase)-	P0450	IHC	Dako Deutschland GmbH

labelled Anti-Rat IgG Ab[#]			
Goat HRP-Labelled Polymer Anti-Mouse Ab[#]	K4001	IHC	Dako Deutschland GmbH
Goat HRP-Labelled Polymer Anti-Rabbit Ab[#]	K4003	IHC	Dako Deutschland GmbH
Goat Alexa Fluor 488 Anti-Mouse IgG Ab[#]	115-546-062	IF	Dianova (Hamburg, Germany)
Chicken Alexa Fluor 594 Anti-Rabbit IgG Ab[#]	A-21442	IF	Invitrogen (Carlsbad, CA, USA)
Goat Alexa Fluor 594 Anti-Rat IgG Ab[#]	A-11007	IF	Invitrogen
Sheep HRP-labelled Anti-Mouse IgG Ab[#]	NA931	WB	GE Healthcare (Little Chalfont, UK)
Donkey HRP-labelled Anti-Rabbit IgG Ab[#]	NA934	WB	GE Healthcare
Donkey HRP-labelled Anti-Goat IgG Ab[#]	sc-2020	WB	Santa Cruz Biotechnology

*Application key: WB = western-blot; IHC = Immunohistochemistry; IF = Immunofluorescence; [**]Reactivity key: H = human; M = mouse; [#]Ab: antibody

Rat cell line and cell culture

The rat pancreatic acinar AR42J cells were purchased from ATCC (CRL-1492, Wesel, Germany). This cell line was cultured in 10 cm dishes in ATCC-formulated F-12K culture medium supplemented with 20% fetal bovine serum (FBS), 100 u/ml penicillin, and 100 µg/ml streptomycin at 37°, 5% CO2. The inhibitor of FGFR, FIIN 1 hydrochloride (10 µM; #3300, Tocris Bioscience, Bristol, UK) was added to proliferating cells for 72 hours. Cells were then lysed and processed for total RNA extraction. For the treatment with Fgf2 (50 ng/ml, 3339-FB-025, R&D systems; Abingdon, UK), growth factors prepared

in F-12K medium containing 5% FBS were added to the proliferating cells for 72 hours in the presence of 10 µg/ml heparin (H3149-10KU, Sigma-Aldrich, St Louis, MO, USA).

RNA isolation

The pancreas tissues were processed according to instructions provided in the RNeasy mini kit (Qiagen, Venlo, Netherlands) using 50 µl of β-mercaptoethanol in 1 ml RLT Buffer. The extracted RNA was eluted in purified water and shock-frozen in liquid nitrogen. Samples were stored at -80°C. The quality of RNA samples was determined by their RINs (RNA Integrity Number; Agilent 2100 Bioanalyzer) which were measured in 59 samples (81%; 59/73). The average RIN of these samples was 6.8, indicating a sufficient RNA quality (Supplementary Table 1). The RIN of 14 samples (labelled as "nd/ok" in Supplementary Table 1) could not be measured due to technical reasons. The RNA quality of these samples was secured by: 1). checking manually whether the presented ribosomal peaks were similar to those RNA samples with RIN more than 5; 2). ruling out significant RNA degradation using electrophoresis on a denaturing agarose gel (Figure S1).

Quantitative Real-Time Polymerase Chain Reaction

Quantitative real time PCR (QRT-PCR) was carried out using the LightCyclerTM480 system with the SYBR Green 1 Master kit (Roche diagnostics, Penzberg, Germany). Expression of the target gene was normalized to the rat housekeeping genes Gapdh (glyceraldehyde-3-phosphate dehydrogenase) or the mouse housekeeping gene Rpl5 (ribosomal protein L5) and Rps29 (ribosomal protein S29) using the LightCyclerTM480 software release 1.5, version 1.05.0.39 (Roche diagnostics).

Microarray gene expression analysis

Gene expression was recorded at different time points after caerulein injections in WT mice, $p48^{Cre/+}$; $Kras^{G12D/+}$ mice and control samples in both mouse strains. An overview of the number of mice, microarray replicates and pathological features at each time point is summarized in Supplementary Tables 2 and 3. Experiments were performed using the Affymetrix GeneChip Mouse Gene 1.0 ST.

Details of normalization, filtering, clustering, PCA, PARAFAC, network and signature analysis are depicted in the Supplementary Methods section.

Immunohistochemistry and immunofluorescence analysis

Harvested tissues were embedded in paraffin and sectioned at 3.5 µm. Sections were subjected to Hematoxylin and eosin (H&E), immunohistolochemical (IHC) and immunoflourescent (IF) staining as described as previously described[1]. For IHC, HRP labelled polymer anti-mouse or anti-rat secondary antibodies (Dako) was applied. For IF, fluorescence-labelled secondary antibodies: goat anti-mouse IgG Alexa Fluor 488 (Dako), goat anti-rat 596 and chicken anti-rabbit 488 (Alexa fluor, Invitrogen, Carlsbad, CA, USA) were used at a dilution of 1:200 and nuclei were counterstained with DAPi. Five non-overlapping images at a 200-fold magnification were acquired per animal.

Serum Analysis

For serum analyses, blood from three to four mice per time point was collected and stored at room temperature for 30 minutes and then centrifuged (5000 g, 20 min, 20°C) for serum collection. Serum levels for amylase, lipase, IL6 and TNFα were measured at the Department of Clinical Chemistry of the Klinikum rechts der Isar of the Technical University Munich, as previously described[2]. Mouse C-reactive protein (CRP) and serum amyloid A (SAA) concentrations were measured using commercially available kits (Mouse C-Reactive Protein/CRP Quantikine ELISA Kit, MCRP00, R&D Systems, Wiesbaden-Nordenstadt, Germany; Mouse Serum Amyloid A ELISA Kit, ab157723, Cambridge, UK) according to the manufacturer's instructions. Importantly, it has been previously reported in the literature that mouse CRP gene may not be active/functional because measured serum concentrations of mouse CRP during acute inflammation are extremely low[3]. Reliable reagents specific for mouse CRP detection have recently become available and have been validated by two independently generated CRP-deficient mouse lines[4 5].

Preparation of acinar explant cultures (3D-cultures)

The 3D-culture was performed as previously described[6]. Briefly, acinar cells from *Kras*^{G12D} or WT mice were isolated from whole pancreatic tissue through collagenase digestion (0.5 mg/ml Collagenase-P, Roche), filtered through a 100 µm nylon cell strainer (BD Biosciences), and washed several times with HBSS (Hanks balanced salt solution, Merck Millipore). Acinar cells were suspended in Waymouth's MB 752/1 medium (Life Technologies GmbH) supplemented with penicillin G, streptomycin, 10% heat-inactivated FBS, 0.1 mg/ml soybean trypsin inhibitor (Sigma Aldrich), 20 µg/ml dexamethasone (Sigma Aldrich), 5 mM HEPES (Life Technologies GmbH), and 0.13% NaHCO3. The cellular suspension was added to neutralized rat tail collagen type I (final concentration 1.5 mg/ml, Corning) and the mixture was solidified at 37°C, 5% CO2. After solidification, supplemented Waymouth's MB 752/1 medium and 50 ng/ml Tgfα (Life Technologies GmbH) was added. Cells were cultivated at 37°C, 5% CO2 for five days. 3D-ADMs were recovered through digestion of the collagen gel with 1 mg/ml collagenase VIII (Sigma Aldrich) RNA isolation.

Quantification

For quantification, images were opened in Windows Paint (Windows 7 Professional, Microsoft Corporation). Every positive cell was marked by a coloured dot by one mouse-click. Mouse-clicks were counted automatically by the Mousometer software of Machart Studios (Machart Studios, Sven Bader, Mannheim, Germany). All images from each individual experiment were quantified simultaneously in order to minimise quantification variation.

Generation of the MADM mouse line

Generation of the MADA mouse line was achieved as previously described[7-9]. Briefly, the MADM cassette was inserted into *Igs2* locus proximal to the p53 locus on mouse chromosome 11. This double marker system requires both MADM-TG and MADM-GT lines that carry a reciprocal mutation at the same locus. The TG line carries a CAG promoter, the N-terminal portion of tdTomato, a loxP-containing intron and the C-terminal portion of mut4-EGFP, whereas the GT line contains a CAG promoter, the N-terminal portion of mut4-EGFP, loxP-containing intron and C-terminal portion of tdTomato tagged with MYC. The homozygous TG line was crossed with the homozygous GT line to generate the trans-

heterozygous TG/GT mutants in which expression of functional fluorescence proteins requires Cre-mediated interchromosomal recombination. This not only re-aligns the respective N- and C- terminus of fluorescence proteins on the same chromosome, but also allows for recombination of more than 99% of genes including p53 on chromosome 11. Previous studies demonstrated that such interchromosomal recombination can be induced in the mitotic (G2), the G1 and the postmitotic (G0) phase (Figure S11A). As for the mitotic events, two types of chromosomal segregations (X and Z segregation) are likely following DNA replication and interchromosomal recombination in the G2 phase: two recombinant sister chromatids segregate into different cells (a G2-X event), producing two single fluorescence-labelled cells; or two recombinant sister chromatids segregate into the same cell (a G2-Z event), producing one double fluorescence-labelled cell and one non-labelled cell (Figure S11A). The G1 and G0 event generated one double fluorescence-labelled cell. Since all these recombination events generate at least one fluorescence-labelled cell, it allows us to precisely follow genetic recombination in the acinar compartment. Importantly, when we introduced a p53-floxed allele into the MADM-11 system (as previously described[8]), the G2-X event would change the genotype of the offspring cells by generating one cell with a double-floxed p53 allele and the other cell with a wild type p53 allele (Figure S11A).

In this study, we observed that EGFP could be visualized by direct fluorescence and IHC staining in fixed pancreatic samples; however, tdTomato could not be seen by direct fluorescence or labelled by antibodies. Because tdTomato is tagged with MYC, anti-MYC antibodies were used for detecting tdTomato-labelled cells.

Microarray gene expression analysis

Experiments were performed using Affymetrix GeneChip Mouse Gene 1.0 ST microarrays, the WT Expression kit (Ambion) and the WT Terminal Labeling and Fragmentation Kit (Affymetrix). Data was normalized and background-corrected using RMA as provided with the Affy package in Bioconductor/R. Genes showing non-significant expression were discarded using the nsFilter function with default parameterization. The remaining set of 20,720 genes was used for all further analysis. Linear models for each gene were constructed using limma. One-way ANOVA followed by empirical Bayes statistics

(eBayes) was performed to identify differentially expressed genes for the previously defined temporal phases.

Clustering

Unsupervised hierarchical clustering (Figure 4A, 4C) was based on the 50% of genes showing the highest variation across all samples in each mouse type separately. Clustering was performed with the complete-linkage method using the Euclidean distance measure using the hclust function in R. PCA (Figure 4B, 4D) was performed using the prcomp function provided with R and was based on the same set of genes used for hierarchical clustering.

Inflammatory (early carcinogenesis) signature

A model for differential expression in the WT inflammatory phase was generated. A gene was selected if its absolute fold change between the wild-type inflammatory phase samples and the wild-type control samples was greater or equal to 2, and the absolute fold change between the wild-type inflammatory phase samples and the wild-type regeneration phase samples was also greater or equal to 2. Samples from the refinement phase were not included due to high intra-sample variance and the small number of samples. Analysis yielded a set of 365 genes (254 up-regulated; 111 down-regulated) with significant differential regulation (absolute FC > 2, adjusted $p < 0.05$) in the inflammation phase of WT mice compared to control samples and regeneration samples (two independent t-tests, Supplementary Figure S8A). A 5-fold cross-validation was applied to generate an “inflammation-specific” signature consisting of 143 genes, allowing for significant differentiation between inflammation phase samples and other samples. The pool of genes obtained showing a specific up-/down-regulation during the inflammatory phase was named the “inflammatory signature".

Hypergeometric testing

Hypergeometric testing was performed multiple times to test for an enrichment of several preselected gene sets within our identified set of differentially expressed genes. Accordingly, the parameters for all

testing procedures were N=20,720, M=365, with "n" referring to the size of the corresponding gene set and "k" referring to the number of hits in each individual case.

Gene regulatory network (GRN) analysis

Microarray data was analyzed based on the previously compiled transcription factor GRN provided by Arda et al[10]. Each gene contained in the network was tested using t-tests for differential expression between the inflammatory phase and the control samples, as well as between the regeneration phase and the control samples. A method provided by Ideker was then applied to derive network subcomponents showing specific activity in the phases[11]. Network subcomponents were scored according to their aggregated z-scores (with respect to the number of nodes and expected average z-score), and optimization was performed with a simulated annealing. The procedure was applied separately for WT and *Kras*^{G12D} mice, respectively.

In vivo PSC-activation signature

An in vitro PSC-activation signature was extracted from a previously published study[12]. It was defined by comparing transcriptomes of preactivated (3-day culture) to culture-activated PSCs (7-day culture) isolated from normal mouse pancreas. The vitro signature was used as a reference to identify PSC-activation signature in vivo from our data set, based on the histological observation that PSC are only activated in the inflammatory phase of WT samples.

PARAFAC analysis

PARAFAC (canonical polyadic decomposition) was applied to the dataset using the implementation included with the R package PTAk. The dataset was restructured into a tensor of dimension 20,720 x 27 x 2 where 27 is the number of samples. Time points that were used for wild-type mice only were rejected for application of this method. Areas of different phases were distinguished using confidence ellipsoids indicating a probability of 95% for respective samples of this phase to be located in this region. Interestingly, 74% (17/23) of *Kras*^{G12D} samples (except for controls) overlap with the confidence ellipsoid of the WT inflammation phase. Additionally, four of the remaining six outlying *Kras*^{G12D}

samples were located closer to the centre of the WT inflammation phase ellipsoid rather than to any other WT ellipsoid. This indicates that 91% (21/23) of the *Kras*^{G12D} samples demonstrate highest similarity in their transcriptome profile to the WT inflammation phase. Remarkably, all ellipsoids from *Kras*^{G12D} samples (except for the controls) overlapped with the WT inflammation phase, which indicates that their transcriptional profiles are not clearly distinguishable.

In silico network modelling

To perform in silico network modelling, we first construct a dual model of the natural inflammatory response and early pancreatic carcinogenesis, as shown in the petri net (Figure 7A). This model consists of four steady states: healthy (control, p_0), inflammation (p_1), regeneration (p_2) and refinement (p_3). Interestingly, and in contrast to wild-type mice (t_0-t_1-t_2-t_3), frequent acinar cell proliferation from 36h on was not seen in early carcinogenesis (t_0-t_1). Because proliferation of progenitor-like cells occurred together with loss of maintenance of the exocrine program in both caerulein-induced inflammation and early carcinogenesis, we hypothesized that these two observations were closely linked and putatively inter-dependent. The previously extracted acinar cell homeostasis genes (see above references; 61 acinar/exocrine homeostasis genes, 22 progenitor genes from embryonic GRN) were used as the backbone for network and interaction construction. This produced a set of 77 preselected genes (6 duplicates). A set of 420 genes (annotated by the GO term ”cell-cell signalling” (GO:0007267)) was used to analysis correlation-based networks for the preselected genes and for genes linked to intercellular signalling. Pearson correlations were computed pair wise between cell-cell signalling genes and preselected genes, and also for pairs of preselected genes between inflammation and regeneration (based on gene expression profiles between 3h and 84h, which marks the transition in proliferation from progenitor-like to acinar cells). Correlation testing followed by Bonferroni correction was performed to derive corrected p-values. This procedure was applied for WT samples and *Kras*^{G12D} samples independently; sample numbers of WT and *Kras*^{G12D} mice were adjusted to allow for a comparative analysis of both networks. All interactions with a corrected p-value smaller than 0.05 were included in the respective networks, yielding a graph with 123 vertices and 296 edges for WT mice, and 14 vertices and 14 edges for *Kras*^{G12D} mice.

Immunohistochemistry and Immunofluorescence

Harvested tissues were conserved overnight in 4% paraformaldehyde (PFA), then embedded in paraffin and cut into 3.5 µm thick slices. Sections were subjected to H&E, IHC and IF, as previously described[13]. Briefly, citric buffer was used for antigen retrieval. IHC staining was performed using 3% BSA (bovine serum albumin, Sigma-Aldrich, Munich, Germany) in PBS as blocking and antibody dilution. IF staining was performed using Triton x100 diluted to 0.6% in PBS plus 3% BSA for blocking, except for Ck19 staining where 10% goat serum in PBS plus 0.6% Triton x100 was used for blocking, primary antibody dilution, and dilution of the secondary antibody.

For quantification IHC pictures, five non-overlapping bright-field images were acquired per animal, resulting in an image size of 355 x 263 µm. Five non-overlapping images were acquired for quantification of IF pictures, resulting in an image size of 697 x 522 µm (for the quantification of proliferating αSMA-positive cells) or an image size of 355 x 263 µm (for the quantification of proliferating α-amylase- and Sox9-positive cells).

References

1. Kong B, Wu W, Cheng T, et al. A subset of metastatic pancreatic ductal adenocarcinomas depends quantitatively on oncogenic Kras/Mek/Erk-induced hyperactive mTOR signalling. Gut 2016;**65**(4):647-57.
2. Miller KJ, Raulefs S, Kong B, et al. Loss of Ifnar1 in Pancreatic Acinar Cells Ameliorates the Disease Course of Acute Pancreatitis. PLoS One 2015;**10**(11):e0143735.
3. Pepys MB. Isolation of serum amyloid P-component (protein SAP) in the mouse. Immunology 1979;**37**(3):637-41.
4. Simons JP, Loeffler JM, Al-Shawi R, et al. C-reactive protein is essential for innate resistance to pneumococcal infection. Immunology 2014;**142**(3):414-20.
5. Teupser D, Weber O, Rao TN, et al. No reduction of atherosclerosis in C-reactive protein (CRP)-deficient mice. J Biol Chem 2011;**286**(8):6272-9.
6. Benitz S, Regel I, Reinhard T, et al. Polycomb repressor complex 1 promotes gene silencing through H2AK119 mono-ubiquitination in acinar-to-ductal metaplasia and pancreatic cancer cells. Oncotarget 2016;**7**(10):11424-33.
7. Zong H, Espinosa JS, Su HH, et al. Mosaic analysis with double markers in mice. Cell 2005;**121**(3):479-92.
8. Liu C, Sage JC, Miller MR, et al. Mosaic analysis with double markers reveals tumor cell of origin in glioma. Cell 2011;**146**(2):209-21.
9. Hippenmeyer S, Youn YH, Moon HM, et al. Genetic mosaic dissection of Lis1 and Ndel1 in neuronal migration. Neuron 2010;**68**(4):695-709.
10. Arda HE, Benitez CM, Kim SK. Gene regulatory networks governing pancreas development. Dev Cell 2013;**25**(1):5-13.
11. Ideker T, Ozier O, Schwikowski B, et al. Discovering regulatory and signalling circuits in molecular interaction networks. Bioinformatics 2002;**18 Suppl 1**:S233-40.
12. Sherman MH, Yu RT, Engle DD, et al. Vitamin d receptor-mediated stromal reprogramming suppresses pancreatitis and enhances pancreatic cancer therapy. Cell 2014;**159**(1):80-93.

13. Kong B, Michalski CW, Hong X, et al. AZGP1 is a tumor suppressor in pancreatic cancer inducing mesenchymal-to-epithelial transdifferentiation by inhibiting TGF-beta-mediated ERK signaling. Oncogene 2010;**29**(37):5146-58.

Supplementary Figures

Supplementary Figure 1:

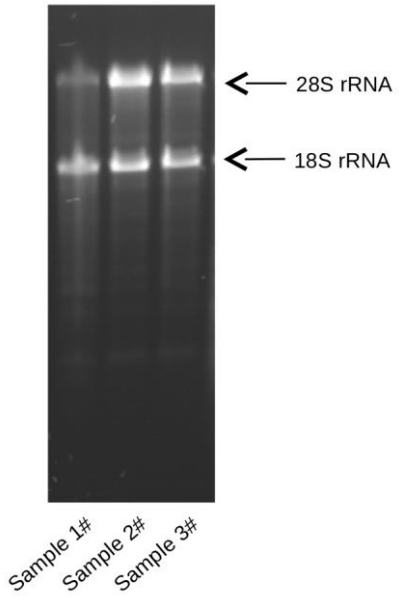

Supplementary Figure 2:

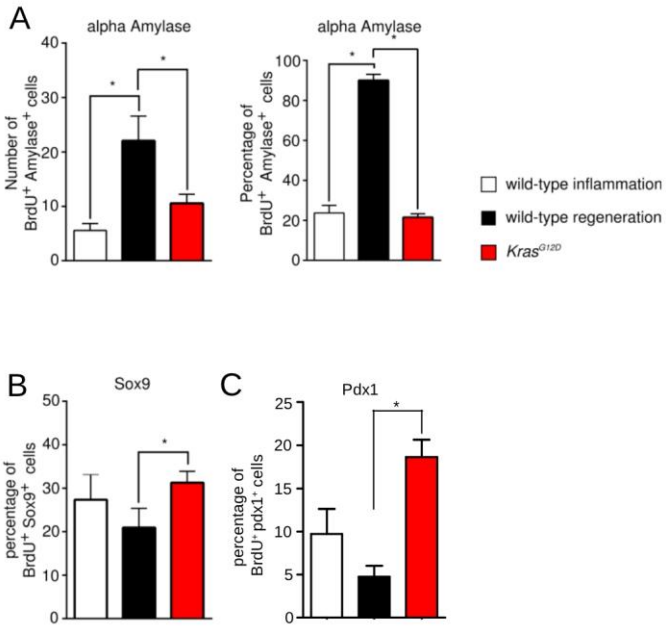

Supplementary Figure 3:

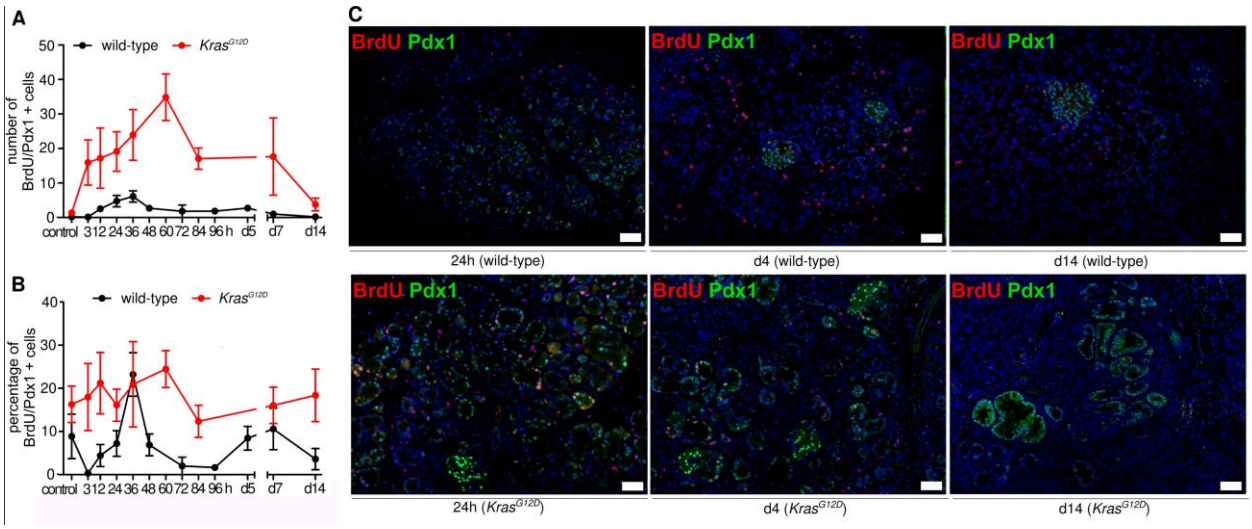

Supplementary Figure 4:

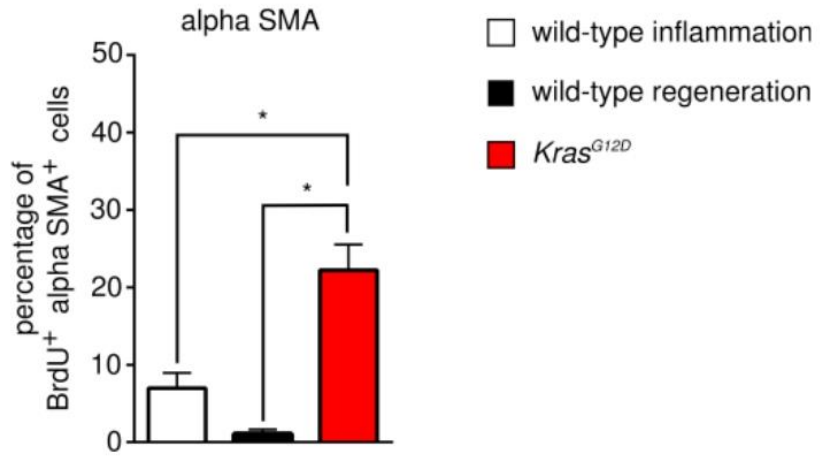

Supplementary Figure 5:

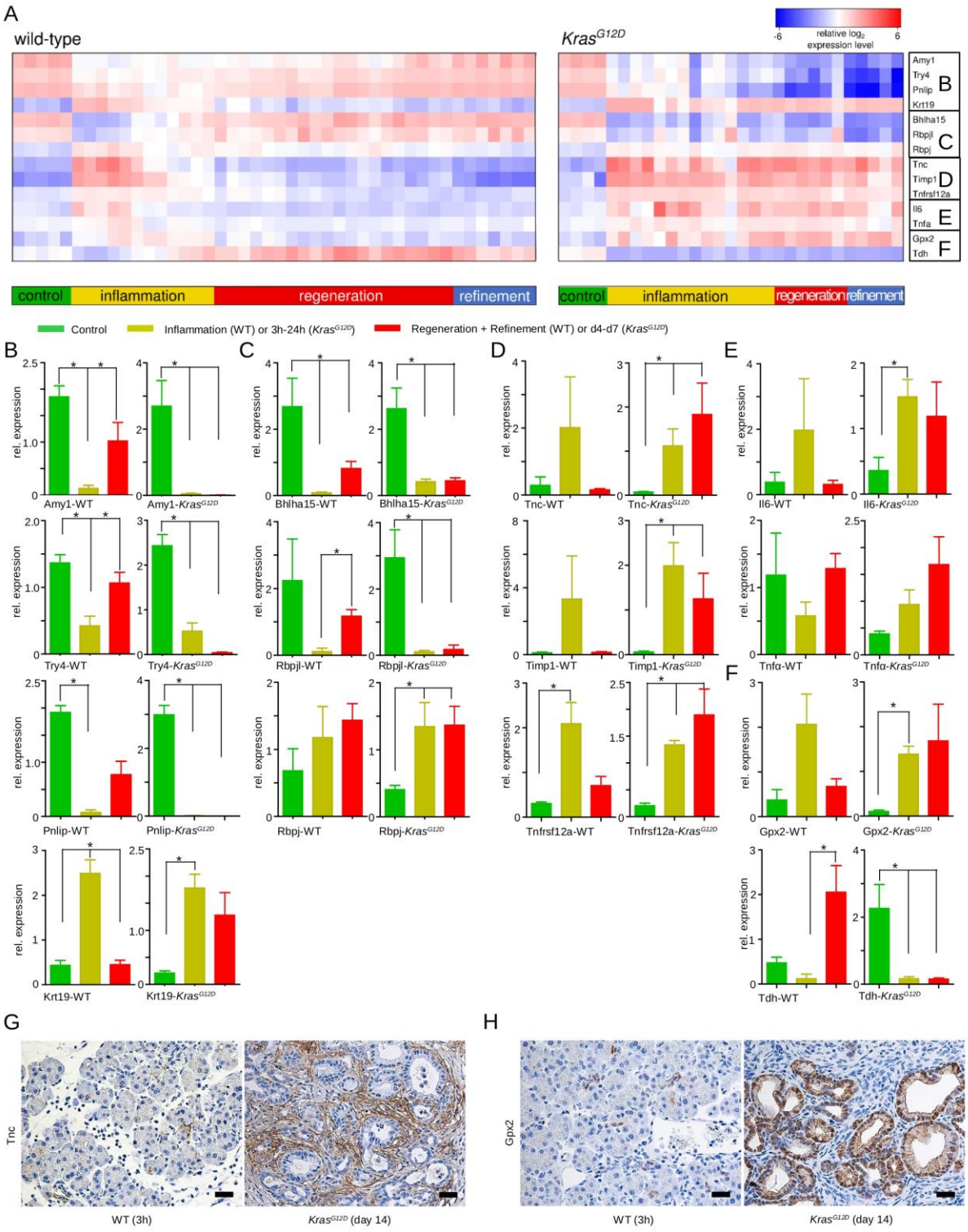

Supplementary Figure 6:

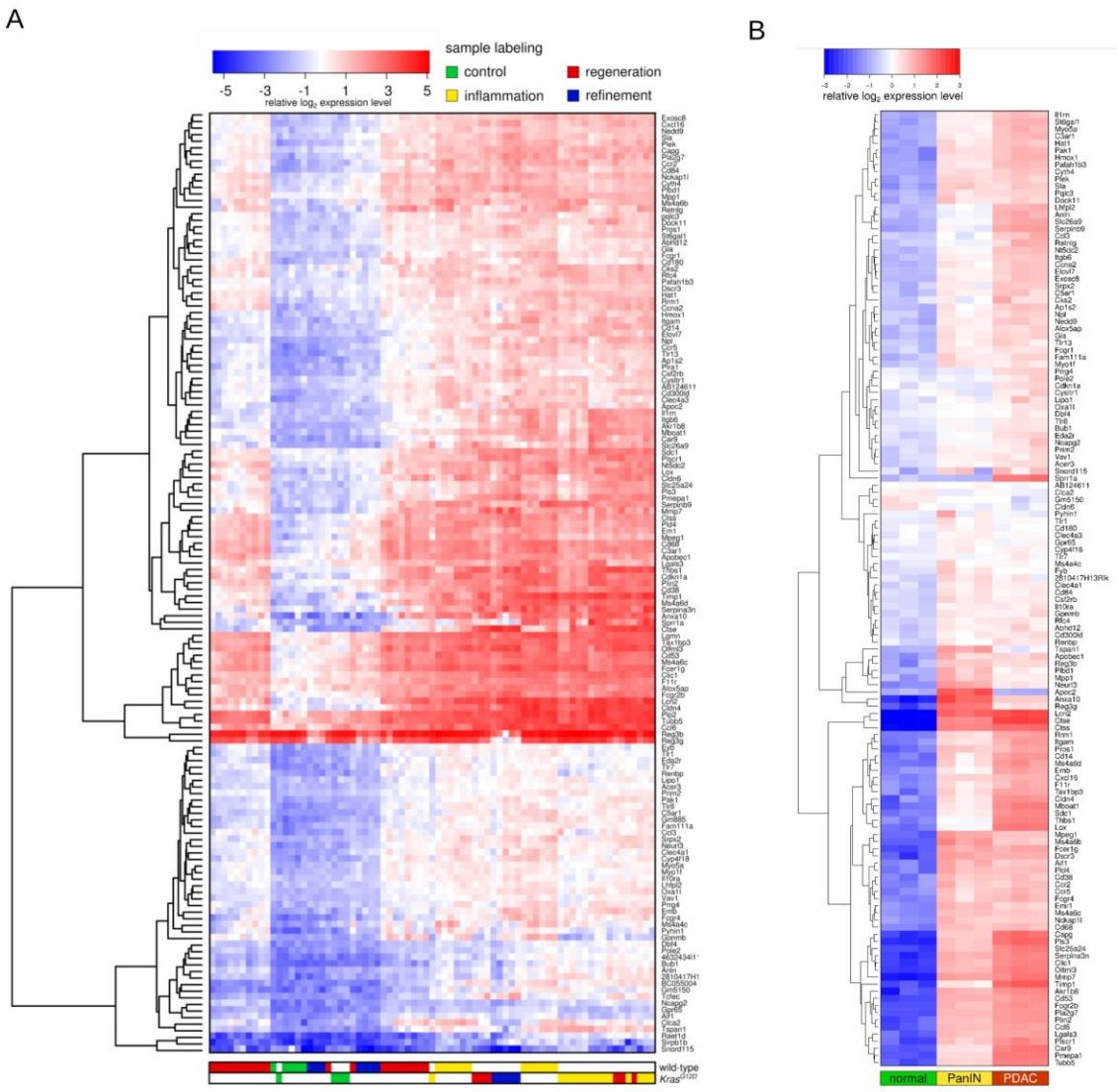

Supplementary Figure 7:

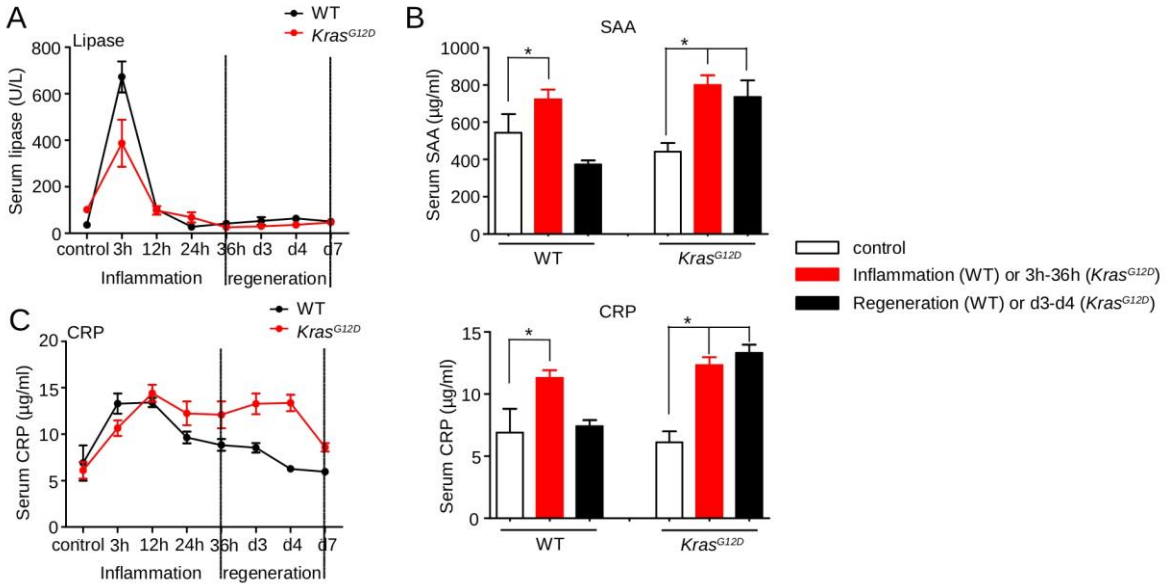

Supplementary Figure 8:

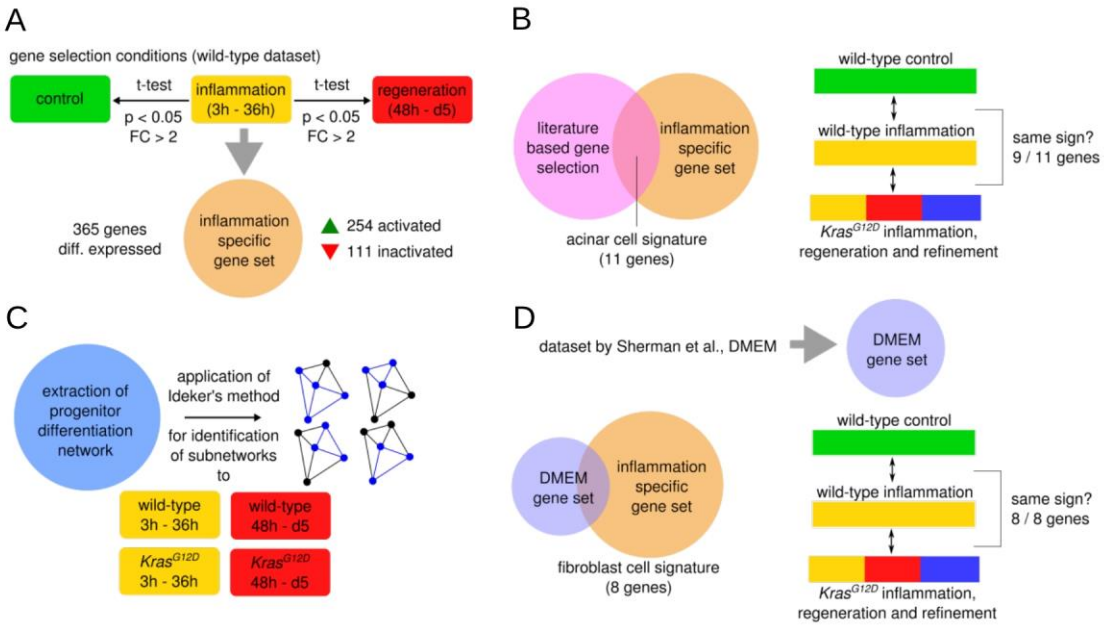

Supplementary Figure 9:

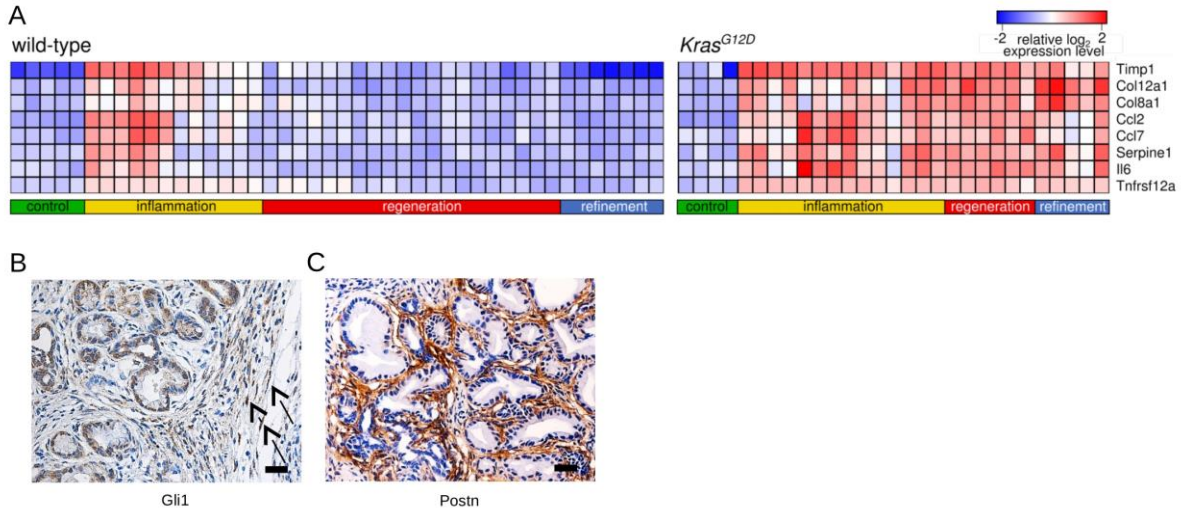

Supplementary Figure 10:

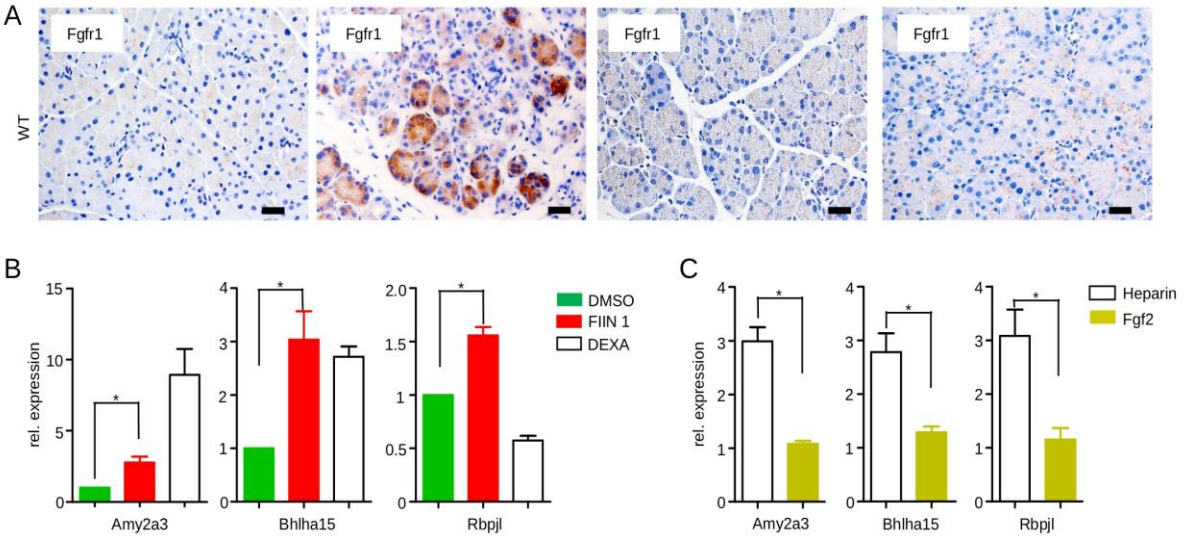

Supplementary Figure 11:

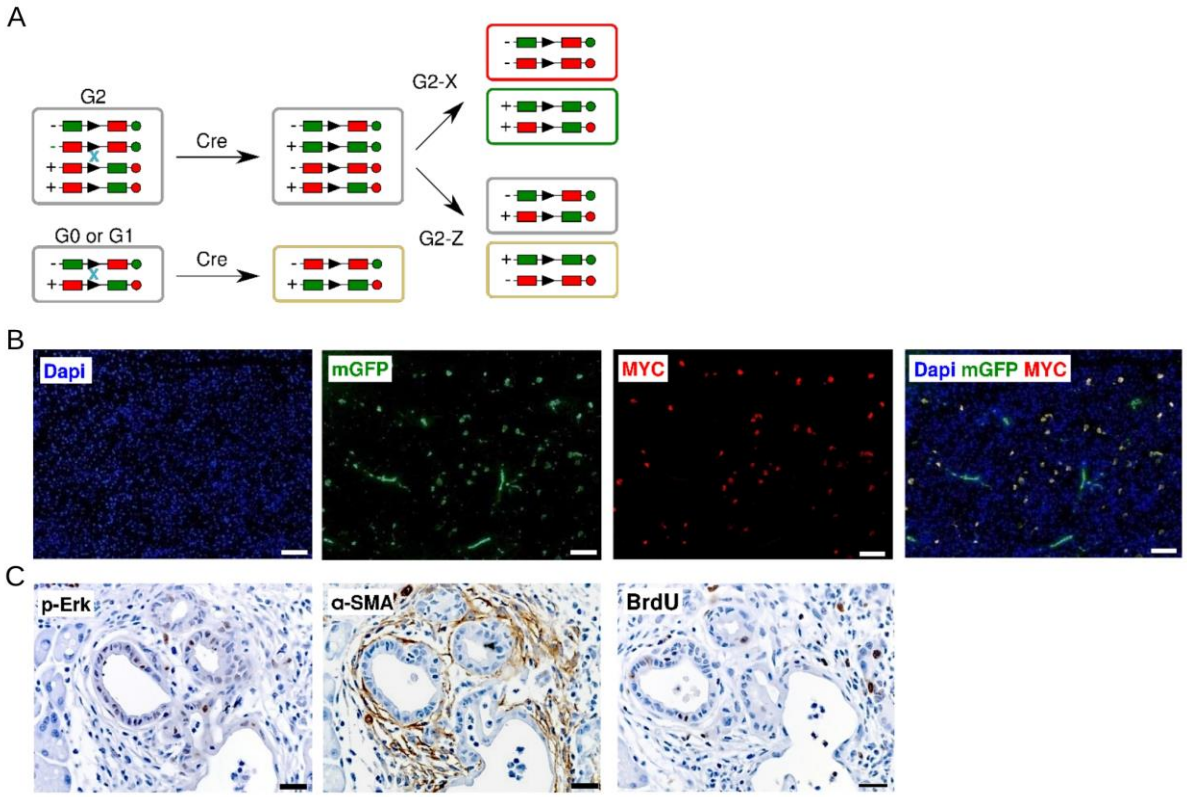

Wild-type	**WT**				
Sample number	**Sample ID**	**Time point**	**RNA ng/µl**	**260/230 ratio**	**RIN***
4R	27.9.13 ctrl12	control	297	2,2	nd/ok
5R	27.9.13 ctrl22	control	723	2,1	5,6
6R	27.9.13 ctrl31	control	379	1,4	nd/ok
1A	Ctrl_2	control	605	1,07	5,8
2A	Ctrl_3	control	505	1,38	5,3
4A	03h_1	3h	1156	1,81	6,0
5A	03h_3	3h	607	1,32	6,3
23C	3h2	3h	659,2	2,2	8,6
7A	12h_1	12h	820	1,51	7,5
8A	12h_2	12h	820	1,4	9,1
9A	12h_3	12h	1322	2,19	8,3
1F	15.08. 24h4	24h	367	1,34	7,1
3F	15.08. 24h2	24h	285	1,98	7,1
2F	15.08. 24h3	24h	244	1,49	6,8
13A	36h_2	36h	411	1,45	7,4
14A	36h_3	36h	432	1,32	7,1
15A	36h_4	36h	731	1,74	8,1
3O	B6 48h1 22.10.12	48h	95,6	1,98	7,2
27C	48h1	48h	201,2	2,21	6,9
29C	48h3	48h	190,2	2,2	6,5
19A	60h_2	60h	166	1,31	8,3
20A	60h_3	60h	191	1,86	6,0
21A	60h_4	60h	205	1,94	6,4
31C	72h1	72h	93,4	2,1	5,7
5P	10-02-13 B6 72h1	72h	307,56	2,19	6,3
6P	10-02-13 B6 72h2	72h	245,48	1,84	4,3
5O	B6 72h2 22.10.12	72h	424,8	2,23	5,6
25A	84h_2	84h	866	2,03	5,0
26A	84h_3	84h	950	2,15	6,3
27A	84h_4	84h	548	2	5,3
36C	96h2	96h	231,3	2,19	6,5
37C	96h3	96h	431,6	2,06	nd/ok
38C	96h4	96h	566,8	1,32	5,9
6O	B6 4.12.12 d51	d5	529	2,1	5,9
7O	B6 4.12.12 d52	d5	453	2,3	6,5
40C	d53	d5	569,7	2	5,4
41C	d54	d5	667,8	1,27	6,9
4F	30.07. d74	d7	1548	1,85	7,1
5F	30.07. d73	d7	1257	2,2	6,8
7F	30.07. d71	d7	449	1,21	6,8
1O	d14 2 B6 25.9.	d14	660,4	2,3	6,9
2O	d14 4 B6 25.9.	d14	821,7	2,32	5,8
1P	4.12.12 d141 b6	d14	162,72	2,29	5,9
2P	4.12.12 d142 b6	d14	381,93	2,26	6,3
$Kras^{G12D}$	**$Kras^{G12D}$**				
Sample number	**Sample ID**	**Time point**	**RNA ng/µl**	**260/230 ratio**	**RIN**
1S	27.9.13 ctrl1	control	342	1,51	nd/ok

2S	27.9.13 ctrl2	control	231	1,1	5,6
3S	27.9.13 ctrl3	control	445	1,6	nd/ok
4S	27.9.13 ctrl4	control	618	2,2	5,6
2D	3h-1	3h-1	1026	2,03	6,6
4E	3.5 3h2	3h	2247		6,9
5E	14.5 3h1	3h	767		7,4
6E	14.5 3h2	3h	1317		7,0
12G	13.8. 12h2	12h	207	2,19	6,2
11G	13.8. 12h1	12h	186	2,26	5,8
1J	3.9. 12h1	12h	942,7	1,3	nd/ok
9E	14.5. 24h1	24h	105		nd/ok
13G	1.8. 24h1	24h	442	2,13	7,2
14G	1.8. 24h2	24h	689	1,17	nd/ok
1Q	10.2.13 kras 24h1	24h	197,37	2,23	nd/ok
5D	36h-1	36h-1	1953	2,15	6,9
2J	3.9. 36h1	36h	625,5	2,23	nd/ok
3J	3.9. 36h2	36h	522	1,64	nd/ok
14E	14.5 48h1	48h	229		8,7
16E	3.5 60h3	60h	928		8,4
7D	60h-1	60h-1	832	2,12	7,8
2Q	10.2.13 kras 60h1 205	60h	59,68	2,24	nd/ok
3Q	10.2.13 kras 60h2 206	60h	238,54	2,3	nd/ok
19E	3.5 84h2	84h	374		7,3
15G	3.7. d72	d7	83	2,19	nd/ok
19G	30.7. d142	d14	62	1,87	7,7
16G	30.7. d73	d7	770	2,39	9,0
17G	13.7. d141	d14	30	0,98	7,7
20G	30.7. d143	d14	495	2,01	9,7

Supplementary Table 1

Table 2: Histological changes after onset of acute pancreatitis in WT mice

Control mice	**1h (n=5)**	**Transcriptional profiles**
	Normal pattern	yes (n=5)
Time point	**3 h (n=13)**	
	Vacuolisation of acinar cells	yes (n=3)
	Single apoptotic acinus cells	
	Initial transformation to tubular complexes (TC)	
Time point	**12 h (n=6)**	
	Acini with larger lumina, more inflammation, initial TC	yes (n=3)
	Less apoptotic cells compared to 3 h	
Time point	**24 h (n=13)**	
	No complete TC, single apoptotic cells, single mitosis	yes (n=3)
	More neutrophile granulocytes	
Time point	**36 h (n=6)**	
	Edema, atrophy of acini, several complete TC	yes (n=3)
	Plenty of apoptosis	
Time point	**48 h (n=15)**	
	Apoptosis and complete TC	yes (n=3)
Time point	**60 h (n=2)**	
	Regeneration,	yes (n=3)
	Mild changes, only few TC, less inflammation, no apoptosis	
Time point	**72 h (n=14)**	
	Small foci with TC (10-15%) and atrophy, regeneration, minimal inflammation	yes (n=4)
Time point	**84 h (n=2)**	
	Single lobuli with TC and atrophy	yes (n=3)
	Regeneration, minimal inflammation	
Time point	**96 h (n=13)**	
	Less atrophie and TC (only small foci) compared to 72 and 84 h	yes (n=3)
Time point	**day 5 (n=16)**	
	Minimal inflammation, only small foci with TC and atrophy	yes (n=4)
Time point	**day 6 (n=2)**	
	Pattern comparable to day 5	
Time point	**day 7 (n=13)**	
	pattern comparable to day 5 and 6; Small foci with TC and atrophy (less than d	yes (n=3)
	Sparse inflammation	
Time point	**day 14 (n=8)**	
	Almost normal pattern, almost complete regeneration	yes (n=4)

Table 3: Acute pancreatitis promotes early carcinogenesis in *Kras*^{G12D} mice

Control mice	1 h (n=4)	Transcriptional profiles
	Focal vacuolisation of acinar cells, Acinar-to-ductal metaplasia (ADM)	yes (n=4)
Time point	**3 h (n=6)**	
	Focal vacuolisation of acinar cells	yes (n=4)
	Dilated/cystic ducts	
Time point	**12 h (n=8)**	
	Acini with larger lumina, More inflammation, Initial TC	yes (n=3)
	Edema, Pancreatic intraepithelial lesions (PanIN I; rare)	
Time point	**24 h (n=5)**	
	Acini with larger lumina, No complete TC, More inflammation + Edema	yes (n=4)
Time point	**36 h (n=9)**	
	Complete TC, Lobular fibrosis	yes (n=3)
	Edema, Less inflammation	
Time point	**48 h (n=1)**	
	Complete TC, Lobular fibrosis, Small areas with intact (regenerated) acinar cells	yes (n=1)
Time point	**60 h (n=9)**	
	Complete TC, Lobular fibrosis, Small areas with intact (regenerated) acinar cells	yes (n=3)
Time point	**72 h**	
		no
Time point	**84 h (n=6)**	
	Complete TC, Lobular fibrosis, Small areas with intact (regenerated) acinar cells	yes (n=3)
	Initial (atypical flat lesions) AFLs	
Time point	**96 h**	
		no
Time point	**day 5**	
		no
Time point	**day 6**	
		no
Time point	**day 7 (n=7)**	
	Lobuli with TC, Initial AFL	yes (n=2)
	Focal lobuli with acinar cell regeneration can be observed	
Time point	**day 14 (n=4)**	
	Lobuli with TC + Fibrosis, AFL	yes (n=3)
	Focal areas with solid AFL high-grade suspicious of initial carcinoma, Lobular architecture preserved, Dilated ducts	

Symbol	Author/Year
Try10l	Masui T/2010
Trypsinogen12	Masui T/2010
Trypsinogen15	Masui T/2010
Gal	Masui T/2010
Prss1	Masui T/2010
Prss3	Masui T/2010
Trypsinogen7	Masui T/2010
Ctrl	Masui T/2010
Try4	Masui T/2010
Prss2	Masui T/2010
Zg16	Masui T/2010
Try5	Masui T/2010
Tff2	Masui T/2010
Zp3	Masui T/2010
Try10	Masui T/2010
Cpb1	Masui T/2010
Cuzd1	Masui T/2010
Ela2a	Masui T/2010
Gatm	Masui T/2010
Hist1h2af	Masui T/2010
Tmed11	Masui T/2010
Klk1b8	Masui T/2010
Cel	Masui T/2010
Sycn	Masui T/2010
Tdh	Masui T/2010
Slc38a5	Masui T/2010
Reg1	Masui T/2010
Slc39a5	Masui T/2010
Pnliprp2	Masui T/2010
Pla2g1b	Masui T/2010
Ela1	Masui T/2010
Gls2	Masui T/2010
Rnase1	Masui T/2010
Spink3	Masui T/2010
Lfng	Masui T/2010
Ppy	Masui T/2010
Fgfbp1	Masui T/2010
Bdh2	Masui T/2010
Ela3b	Masui T/2010
Tmem54	Masui T/2010
Vtn	Masui T/2010
Serinc3	Masui T/2010
Pnliprp1	Masui T/2010
Reg3d	Masui T/2010
Pkig	Masui T/2010
Dmbt1	Masui T/2010
Upk1a	Masui T/2010
Ttc9	Masui T/2010
Klk1	Masui T/2010
Agr2	Masui T/2010
Derl3	Masui T/2010

Gcat	Masui T/2010
Slc6a9	Masui T/2010
Bhlha15	Masui T/2010
Xbp1	Masui T/2010
Nr5a2	Masui T/2010
Hnf1a	Direnzo/2012
Gata6	Lee AH/2005
Rbpj	von Figura G/2014
Rbpjl	Molero X/2012
Ptf1a	Martinelli P/2013

supplementary Table 4

Table 5: List of genes associated with the inflammatory phase

ID	inflamm.ctrl	adj.P.Val	inflamm.reg	adj.P.Val
Bhlha15	-2,349839	1,65E-10	-2,19437	7,50E-10
Rbpjl	-1,502909	2,14E-06	-1,357284	9,82E-06
Tff2	-2,314308	1,01E-16	-1,61439	9,88E-13
Cuzd1	-1,239757	5,01E-09	-1,240629	4,13E-09
Tmed11	-4,192618	2,79E-13	-2,319518	2,62E-07
Gal	-3,242082	1,12E-12	-2,226483	9,06E-09
Slc38a5	-2,722626	1,67E-11	-1,95579	3,19E-08
Ttc9	1,9890301	9,34E-09	1,120576	0,0001746
Agr2	-3,409335	7,88E-10	-3,923266	2,67E-11
Slc39a5	-2,534775	2,91E-12	-1,722987	2,45E-08
Derl3	-2,878702	1,75E-11	-2,834915	2,67E-11